

OPTICAL MODE DISTORTION IN A SHORT RAYLEIGH LENGTH FREE ELECTRON LASER

J. Blau, W.B. Colson, B.W. Williams, S.P. Niles and R.P. Mansfield
Physics Department, Naval Postgraduate School
333 Dyer Road, Monterey, CA 93943

Abstract

A short-Rayleigh length free electron laser (FEL) will operate primarily in the fundamental mode with a Gaussian profile that is narrow at the waist and broad at the mirrors. The gain medium will distort the optical wavefront and produce higher-order modes that will expand more rapidly than the fundamental. Wavefront propagation simulations are used to study optical mode distortion, as electron beam, undulator, and optical cavity parameters are varied.

INTRODUCTION

A proposed design for a high-power free electron laser calls for a short-Rayleigh length optical cavity [1]. This design has several advantages. The strongly-focused optical mode is narrow at the waist, enhancing the interaction with the electron beam. The small interaction volume should improve optical beam quality, encouraging the development of a fundamental Gaussian mode. The rapidly-expanding mode will reduce the peak intensity on the cavity mirrors, lessening the possibility of mirror damage.

The narrow, high-current electron beam will distort the optical mode, as new light is created due to spontaneous and stimulated emission along the length of the undulator. Higher-order modes may develop, and propagate to the cavity mirrors. Some power may be lost outside the mirrors, but the portion that remains within the cavity will produce a combined wavefront that no longer has a simple Gaussian profile.

SHORT-RAYLEIGH LENGTH FEL PARAMETERS

A proposed high-power FEL has electron beam energy $E_b = 80$ MeV, bunch charge $q = 200$ pC and bunch length $l_b = 0.15$ mm, yielding a peak current of $\hat{I} = 400$ A. The normalized emittance is $\epsilon_n = 3$ mm-mrad, with a beam radius of $r_b = 60$ μ m. The undulator consists of $N = 22$ periods, each of length $\lambda_0 = 2.36$ cm, for a total length of $L = 52$ cm, with a peak magnetic field $\hat{B} = 0.7$ T. The undulator parameter is $K = 1$. The optical cavity is $S = 18$ m long, with Rayleigh length $Z_0 = 6$ cm, and quality factor $Q_n = 4$, corresponding to 25% power transmission per pass. The optical wavelength is $\lambda = 1$ μ m.

Our simulations use dimensionless parameters [2]. Longitudinal distances are normalized to the undulator length L , and transverse distances are normalized to $(L\lambda/\pi)^{1/2}$.

The dimensionless current density is given by

$$j = \frac{8N(e\pi KL)^2 \rho_e}{\gamma^3 mc^2}, \quad (1)$$

where $\rho_e \propto \hat{I}$ is the electron particle density, $\gamma = E_b/mc^2$ is the Lorentz factor, e and m are the electron charge and mass, and c is the speed of light. For the above parameters, $j = 200$. The dimensionless electron beam radius is $\sigma = r_b/(L\lambda/\pi)^{1/2} = 0.15$ and the dimensionless Rayleigh length is $z_0 = Z_0/L = 0.12$. The dimensionless cavity length is $\tau_{\text{mirror}} = S/L = 35$.

SIMULATION METHOD

Our wavefront propagation program has been described elsewhere [3]. At each time step, it uses the relativistic Lorentz force equations to determine the electron motion in the presence of the undulator and optical fields, and the parabolic wave equation to evolve the optical wavefront in (x, y, t) . The simulation can follow multiple and arbitrary transverse optical modes, as they interact with the electron beam and bounce back and forth in the optical cavity, including mirror transmission and edge losses. We typically start the simulation in weak optical fields, and allow it to evolve over many passes through the cavity until the FEL reaches steady-state.

Recent improvements to our program include a faster Fourier transform algorithm [4], a more accurate integration method that uses next-nearest neighbors in the propagation of the wavefront matrix, and an expanding coordinate system to follow the rapidly-diffracting optical mode with a reasonable grid size [5].

SIMULATION RESULTS

For each set of simulation runs described below, we start with the nominal parameters given above. Then we vary some of the parameters to determine the effect on FEL performance and optical beam quality.

Fig. 1 shows the steady-state extraction for many simulations as the current density j is varied while emittance is held constant. Extraction is defined as the fraction of electron beam power converted to optical power on a single pass through the undulator. A theoretical curve, discussed below, is also shown for reference.

Since the weak-field gain is proportional to j , there is a minimum threshold value of $j \approx 20$ below which there is no extraction, because the cavity losses exceed the gain. For larger values of j , the power will grow over each pass

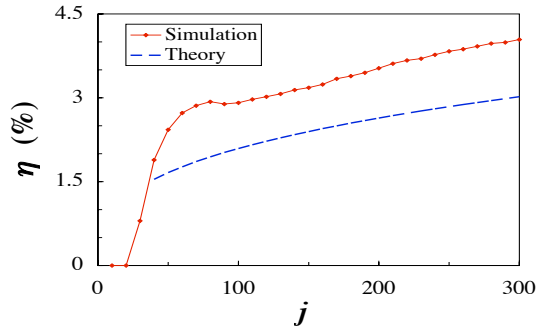


Figure 1: Extraction η versus current density j , for a series of simulations (solid red line), compared to theory (dashed blue line).

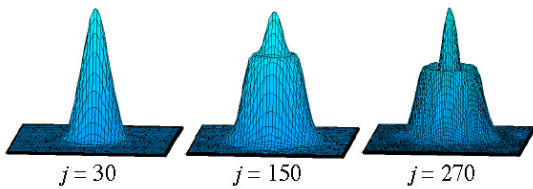


Figure 2: Optical field amplitude $|a(x, y)|$ at the output mirror for several values of current density j .

until the laser reaches saturation in strong optical fields. Basic FEL theory [2] predicts that for high gain, $j \gg 1$, the extraction should grow as

$$\eta \approx \frac{(j/2)^{1/3}}{8N}. \quad (2)$$

Eq. 2 is plotted as a dashed blue line in Fig. 1. The similar slope of the two curves confirms the $j^{1/3}$ dependence, but the theory curve is well below the simulation curve. However, Eq. 2 is only an approximation, and doesn't include the effects of mode distortion.

Fig. 2 shows the steady-state optical wavefront profile at the output mirror for several values of j . For low current, $j = 30$, the laser appears to be operating close to the fundamental mode. For moderate current, $j = 150$, the mode is beginning to distort. For high current, $j = 270$, there is at least one higher-order Laguerre-Gaussian mode evident. This series clearly shows the effect of the FEL gain medium on mode distortion.

Fig. 3 shows the results of many simulations as the electron beam radius σ is varied. The beam angular spread is also varied to keep the emittance constant. For small beam radii, the corresponding large angular spread reduces overlap with the optical beam over the length of the undulator, hence lowering extraction. For large beam radii, many electrons are outside the strongly focused optical beam at the waist, again reducing extraction. The simulations predict that the optimal beam radius is at $\sigma = 0.12$.

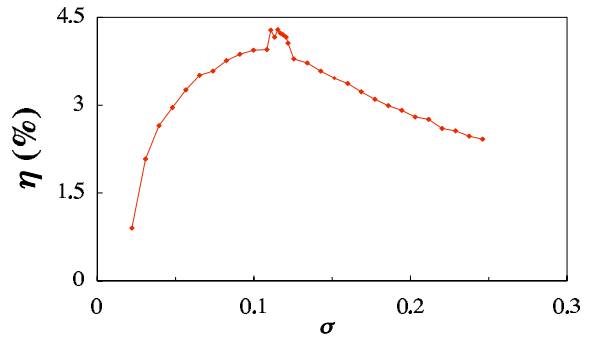


Figure 3: Simulation results for extraction η versus electron beam radius σ .

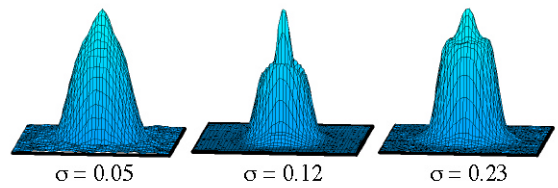


Figure 4: Optical field amplitude $|a(x, y)|$ at the output mirror for several values of electron beam radius σ .

There is a curious feature in the center of Fig. 3, around $\sigma \approx 0.12$, where the extraction appears to briefly rise a bit higher than the overall trend. This may be due to optical mode distortion around that value. Fig. 4 shows the output wavefront for several values of σ .

We also consider varying the electron beam focus point from $\tau_\beta = 0 - 1$, normalized to the undulator length L . The simulations give a fairly constant extraction over the entire range, as shown in Fig. 5, predicting that the short-Rayleigh length FEL should be fairly insensitive to fluctuations in the electron beam focal point. The optical mode profiles (not shown) do not change much over this range.

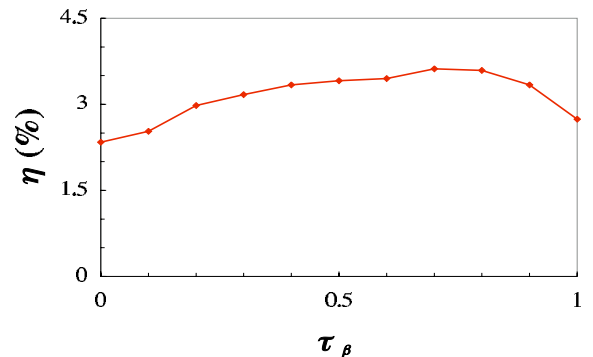


Figure 5: Simulation results for extraction η versus electron beam focus position τ_β within the undulator.

Next, we look at the effects of varying the number of

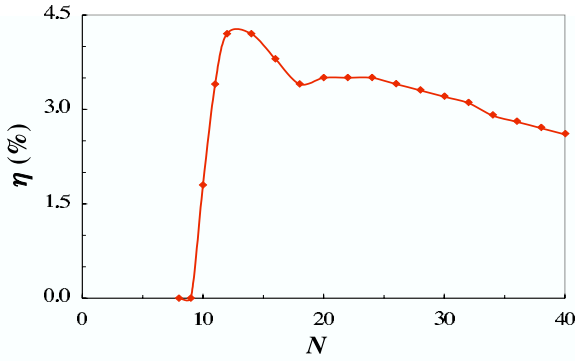


Figure 6: Simulation results for extraction η versus number of undulator periods N .

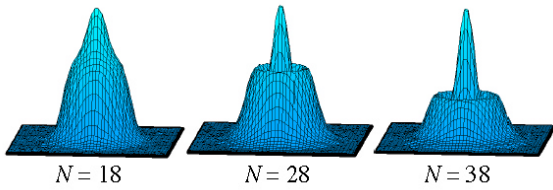


Figure 7: Optical field amplitude $|a(x, y)|$ at the output mirror for various number of undulator periods N .

undulator periods N , keeping the undulator period λ_0 constant. The simulation results are plotted in Fig. 6. Note that changing N affects many other dimensionless parameters; for example, the electron current density $j \propto N^3$. Consequently, if there are too few periods, the gain will be below threshold, and the simulation results indeed show that there is no extraction for $N < 10$, corresponding to $j < 20$. Above that, the extraction increases rapidly, until $N \approx 14$. For larger values of N , even though j continues to increase, the extraction drops off. The optical wavefronts in Fig. 7 predict the development of higher-order modes as N increases.

The results for undulator length motivate consideration of tapering the undulator, to extend saturation and enhance extraction. Fig. 8 shows simulation results as the undulator taper rate is varied. The taper rate is defined by

$$\delta \approx -4\pi N \left(\frac{K^2}{1+K^2} \right) \frac{\Delta K}{K}, \quad (3)$$

where $\Delta K/K$ is the change in the undulator parameter. The simulations confirm that a positive taper could significantly improve FEL performance. A taper rate of $\delta = 11\pi$ produced an extraction of 5.9%, compared to the untapered value of 3.4%. Tapering also seems to improve the beam quality. Fig. 9 shows the output wavefront for several taper values; at $\delta = 11\pi$ it is close to the fundamental mode.

Next we show a series of simulations varying the Rayleigh length from $z_0 = 0.05 - 0.85$, normalized to the undulator length L . The results are shown in Fig. 10.

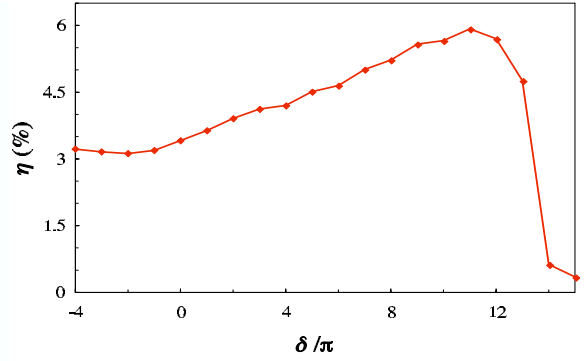


Figure 8: Simulation results for extraction η versus undulator taper strength δ .

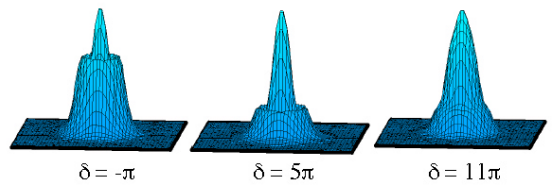


Figure 9: Optical field amplitude $|a(x, y)|$ at the output mirror for several values of undulator taper strength δ .

The extraction changes very little over this entire range, confirming that a short-Rayleigh length FEL can maintain good extraction while reducing optical intensity on the mirrors. Fig. 11 shows the output wavefronts at several values of z_0 . Note that these are not all drawn to the same scale since the beam width expands as z_0 decreases.

Finally, we vary the cavity length over the range $\tau_{mirr} = S/L = 5 - 35$. The mirror curvature is also changed to keep z_0 constant. Again there is little variation in the extraction, as shown in Fig. 12, although the optical mode profiles, as shown in Fig. 13 become increasingly distorted as the cavity is lengthened. Again, these are not all drawn to the same scale; the beam width expands dramatically as τ_{mirr} increases.

ACKNOWLEDGMENTS

The authors are grateful for the support from NAVSEA, ONR, and the JTO.

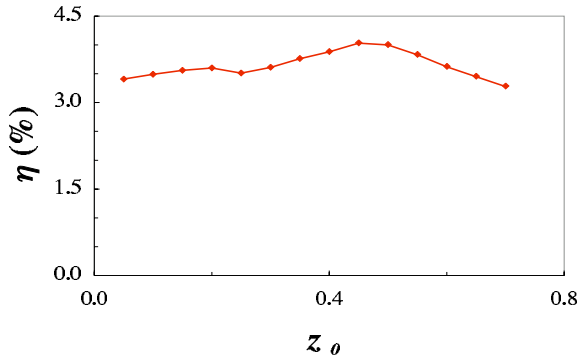


Figure 10: Simulation results for extraction η versus Rayleigh length z_0 .

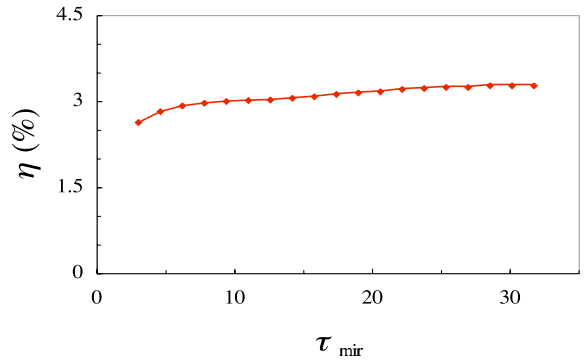


Figure 12: Simulation results for extraction η versus cavity length τ_{mirr} .

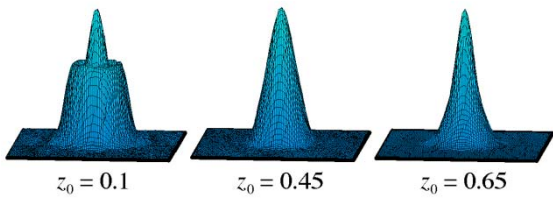


Figure 11: Optical field amplitude $|a(x, y)|$ at the output mirror for several values of Rayleigh length z_0 .

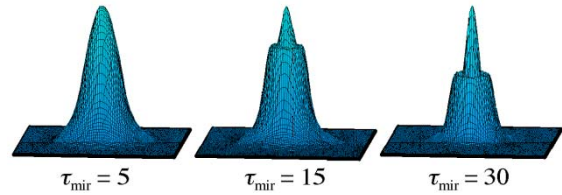


Figure 13: Optical field amplitude $|a(x, y)|$ at the output mirror for several values of cavity length τ_{mirr} .

REFERENCES

- [1] W.B. Colson, "Short Rayleigh length free electron lasers", Proc. FEL2004.
- [2] W.B. Colson, in: W.B. Colson, C. Pellegrini, A. Renieri (Eds.), Laser Handbook, Vol. 6, North Holland, Amsterdam, 1990.
- [3] J. Blau, Ph.D. Dissertation, Naval Postgraduate School, <http://handle.dtic.mil/100.2/ADA401739> (2002).
- [4] Frigo, Matteo and Johnson, "FFTW: An adaptive software architecture for the FFT", Proc. 1998 Intl. Conf. Acoustics Speech and Signal Processing, 1381 (1998).
- [5] R.L. Armstead, J. Blau, and W.B. Colson, "Short Rayleigh length free electron laser simulations in expanding coordinates", Proc. FEL2004.